Two dimensional electron gases induced by spontaneous and piezoelectric polarization in undoped and doped AlGaN/GaN heterostructures

O. Ambacher,[a] B. Foutz, J. Smart, J. R. Shealy, N. G. Weimann, K. Chu, M. Murphy, A. J. Sierakowski, W. J. Schaff, and L. F. Eastman
School of Electrical Engineering, Cornell University, Ithaca, New York 14853

R. Dimitrov, A. Mitchell, and M. Stutzmann
Walter Schottky Institute, TU-Munich, Am Coulombwall, D-85748 Garching, Germany

(Received 10 May 1999; accepted for publication 19 September 1999)

Two dimensional electron gases in $Al_xGa_{1-x}N$/GaN based heterostructures, suitable for high electron mobility transistors, are induced by strong polarization effects. The sheet carrier concentration and the confinement of the two dimensional electron gases located close to the AlGaN/GaN interface are sensitive to a large number of different physical properties such as polarity, alloy composition, strain, thickness, and doping of the AlGaN barrier. We have investigated these physical properties for undoped and silicon doped transistor structures by a combination of high resolution x-ray diffraction, atomic force microscopy, Hall effect, and capacitance–voltage profiling measurements. The polarization induced sheet charge bound at the AlGaN/GaN interfaces was calculated from different sets of piezoelectric constants available in the literature. The sheet carrier concentration induced by polarization charges was determined self-consistently from a coupled Schrödinger and Poisson equation solver for pseudomorphically and partially relaxed barriers with different alloy compositions. By comparison of theoretical and experimental results, we demonstrate that the formation of two dimensional electron gases in undoped and doped AlGaN/GaN structures rely both on piezoelectric and spontaneous polarization induced effects. In addition, mechanisms reducing the sheet carrier concentrations like nonabrupt interfaces, dislocations, and the possible influence of surface states on the two dimensional electron gases will be discussed briefly. © *2000 American Institute of Physics.* [S0021-8979(00)03401-0]

I. INTRODUCTION

AlGaN/GaN high electron mobility transistors (HEMTs) have been a subject of intense recent investigation and have emerged as attractive candidates for high voltage, high-power operation at microwave frequencies.[1–7] Although the maximum electron drift mobility of two dimensional electron gases with sheet carrier concentrations of about $5\times10^{12}\,cm^{-2}$ in GaN is predicted to be about 2000 and 18 000 $cm^2/V\,s$ at 300 and 77 K, respectively, which is much less than that of GaAs, GaN has a larger peak electron velocity, larger saturation velocity, higher breakdown voltage, and thermal stability, making this material very suitable for use as channel material in microwave power devices.[8–11] Further contributing to the outstanding performance of AlGaN/GaN based HEMTs is the ability to achieve two dimensional electron gases (2DEGs) with sheet carrier concentrations of up to $2\times10^{13}\,cm^{-2}$ close to the interface, well in excess of those observed in other III–V material systems. These high sheet carrier concentrations enable the fabrication of AlGaN/GaN based HEMTs with channel currents above 1000 mA/mm, breakdown voltages of 140 V (for a gate length of 0.8 μm), and cutoff frequencies of $f_t=68$ GHz and $f_{max}=140$ GHz (for a gate length of 0.15 μm).[12] With high structural quality heterostructures grown on c-Al_2O_3 or SiC substrates, high output powers of 4 and 12 W/mm, respectively, together with high power added efficiency (60%–70%) are predicted.[12] Large periphery AlGaN/GaN based devices have been fabricated on SiC recently, which demonstrated power densities and total powers of 6.9 W/mm and 9.1 W at a frequency of 10 GHz.[13]

It has been shown previously that piezoelectric effects can exert a substantial influence on the concentration and distribution of free carriers in strained group-III nitride heterostructures with the wurtzite crystal structure grown in the (0001) orientation.[14–16] This is further emphasized in pseudomorphic, wurtzite AlGaN/GaN based transistor structures, where the piezoelectric polarization of the strained AlGaN barrier layer is more than five times that of AlGaAs/GaAs structures. Polarization induced electric fields lead to a significant increase of the sheet carrier concentration and narrower confinement of the 2DEG.[17–20] Bernardini *et al.* predicted that, in addition to the high piezoelectric polarization, the spontaneous polarization (polarization at zero strain) is very large in wurtzite group-III nitrides, increasing from GaN over InN to AlN,[21] resulting in a further increase of polarization induced effects in AlGaN/GaN based HEMTs.

In this article we will focus on the electrical and structural characterization of strained AlGaN/GaN heterostructures grown by metalorganic chemical vapor deposition (MOCVD) or plasma induced molecular beam epitaxy (PIMBE) to understand the formation of 2DEGs in undoped

[a]Electronic mail: ambacher@wsi.tu-muenchen.de

and doped HEMTs induced by spontaneous and piezoelectric polarization. High resolution x-ray diffraction, capacitance–voltage ($C-V$) profiling, and Hall effect measurements have been used to determine the thickness, strain, and alloy composition of the AlGaN barrier, as well as the sheet carrier concentration of the 2DEGs. In addition the sheet charge bound at the AlGaN/GaN interface induced by polarization effects will be calculated from different sets of piezoelectric constants available in the literature. The uncertainty in the determination of the polarization induced sheet charge and in turn the estimated 2DEG density due to the limited precision of the piezoelectric constants will be discussed. The measured sheet carrier concentrations of the 2DEGs will be compared with self-consistent calculations from a coupled Schrödinger and Poisson equation solver over a broad range of alloy compositions for undoped and doped HEMT structures. Furthermore, physical properties causing a reduction of the 2DEG sheet carrier concentration such as the degree of relaxation of the barrier, dislocations, and surface states will be addressed.

II. GROWTH OF UNDOPED AND DOPED AlGaN/GaN HETEROSTRUCTURES

The investigated epitaxial AlGaN/GaN and GaN/AlGaN/GaN HEMT structures were grown by MOCVD or PIMBE on *c*-plane sapphire substrates. The MOCVD grown undoped AlGaN/GaN heterostructures were deposited at a pressure of 100 mbar, using triethylgallium, trimethylaluminium, and ammonia as precursors. A growth rate of about 0.5 μm/h was achieved for a substrate temperature of 1040 °C at V/III gas phase ratios of 1800 and about 900 for GaN and AlGaN, respectively.[22] The AlGaN/GaN heterostructure as well as the $Al_{0.1}Ga_{0.9}N$ nucleation layer were grown at a constant substrate temperature and without any growth interruptions to avoid the presence of excessively high free carrier background concentrations. $Al_xGa_{1-x}N$ barriers with thicknesses between 100 and 450 Å and alloy compositions of up to $x=0.45$ were deposited on GaN buffer layers with thicknesses between 1 and 2.5 μm. Atomic force microscopy (AFM) scans showed a crack free surface morphology with bilayer steps causing a root mean square surface roughness as low as 0.2 nm for HEMT structures grown using AlGaN nucleation layers with a thickness of about 20 nm. The Ga-face polarity of the MOCVD grown GaN buffer layer and transistor structures was inferred from x-ray standing wave measurements and wet chemical etching (discussed in more detail in Refs. 16 and 23). The 2DEG mobility for HEMTs with 300 Å $Al_{0.3}Ga_{0.7}N$ barriers was determined to be 1496 (300 K), 4436 $cm^2/V\,s$ (77 K), and 1575 (300 K), 7520 $cm^2/V\,s$ (77 K) for buffer layer thicknesses of 1.1 and 2.2 μm, respectively. The improved mobility is attributed to the improved structural quality of the AlGaN/GaN interface with increasing thickness of the GaN buffer.[16]

Undoped and doped GaN/AlGaN/GaN heterostructures were deposited on c-Al_2O_3 substrates by PIMBE using conventional effusion cells, and a radio frequency plasma source for the generation of nitrogen radicals. The nitrogen flux through the plasma source was fixed at 2 sccm causing a nitrogen partial pressure in the MBE chamber of 4×10^{-5} mbar during growth. The optimized growth temperature for GaN was determined to be between 780 and 800 °C for a Ga flux towards the sample surface of $1.5\times10^{15}\,cm^{-2}\,s^{-1}$ resulting in a growth rate of 0.5 μm/h. As discussed in more detail in Ref. 24, GaN grown on sapphire substrates without a special approach to form a nucleation layer was determined to be N-face. Epitaxial GaN layers with N-face polarity grown by PIMBE exhibited a x-ray diffraction peak with a FWHM of 250 arcsec [rocking curve of (0002) reflex] and a surface roughness rms <2 nm for 2.5 μm thick films. The free carrier concentration of N-face GaN was reduced from 1×10^{17} to below $5\times10^{14}\,cm^{-3}$ by intentional doping with magnesium acceptors.[25]

By depositing a 7–10 nm thick AlN nucleation layer at a growth rate and substrate temperature of 0.35 μm/h and 800 °C, respectively, prior to growth of the GaN buffer layer, the polarity of the heterostructure was changed to Ga-face. It should be mentioned that a complete coverage of the substrate surface by the AlN nucleation layer is essential to grow high quality Ga-face GaN by PIMBE, as was confirmed by transmission electron microscopy. Incomplete coverage of the substrate surface by AlN results in a GaN buffer layer of mixed polarity. The structural quality of the Ga-face in comparision to N-face heterostructures was found to be higher.[24] The surface roughness of the Ga-face GaN was below 1 nm and compensation by magnesium acceptors was not necessary to achieve insulating films. AlGaN barriers with thicknesses between 200 and 1000 Å were grown on GaN buffer layers with N-face or Ga-face polarity using the optimized flux of Ga–metal atoms for the total flux of group-III atoms. Crack free barriers with alloy compositions of up to $x=0.65$ were realized and capped with a 20 or 300 Å GaN layer for Ga- and N-face heterostructures, respectively. To enable a comparison of 2DEGs formed in undoped and doped N-face GaN/AlGaN/GaN heterostructures, samples were grown with silicon doped AlGaN barriers. The barrier layers were doped over a depth between 100 and 200 Å with a silicon concentration of about $10^{19}\,cm^{-3}$ leaving a spacer layer of 30 Å from the AlGaN/GaN interface.

For N-face heterostructures, the highest 2DEG mobility of 1150 (300 K) and 3450 $cm^2/V\,s$ (77 K) was achieved for a 400 Å thick undoped barrier with an Al concentration of $x=0.25$, causing an electron sheet carrier concentration of $5\times10^{12}\,cm^{-2}$ at the GaN/AlGaN interface. Higher mobilities of 1432 (300 K) and 3900 $cm^2/V\,s$ (77 K) at a sheet carrier concentration of $1.3\times10^{13}\,cm^{-2}$ at the AlGaN/GaN interface were observed for Ga-face heterostructures with a barrier thickness of 200 Å and an alloy composition of $x=0.35$, demonstrating the better electron transport properties for Ga-face heterostructures.[8,16]

To understand the formation of 2DEGs with extremely high sheet carrier concentrations above $10^{13}\,cm^{-2}$ observed in undoped as well as in doped AlGaN/GaN heterostructures, we have to discuss the role of piezoelectric and spontaneous polarization effects in group-III nitride heterostructures.

III. POLARIZATION INDUCED SHEET CHARGE

The wurtzite group-III nitrides InN, GaN, and AlN are tetrahedrally coordinated semiconductors with a hexagonal

Bravais lattice with four atoms per unit cell.[1] Their crystal lattice structure can be defined by the length of the hexagonal edge a_0, the height c_0 of the prism, and a microscopic dimensionless parameter u, which is defined as the length of the bond parallel to the c axis (parallel to [0001]), in units of c_0. The piezoelectric tensor has three independent components (C_{6v} point group). Two of these components measure the piezoelectric polarization P_{PE} induced along the c axis or in the basal plane. The relevant relationship is

$$P_{PE}=e_{33}\epsilon_z+e_{31}(\epsilon_x+\epsilon_y), \tag{1}$$

where $\epsilon_z=(c-c_0)/c_0$ is the strain along the c axis, the in-plane strain $\epsilon_x=\epsilon_y=(a-a_0)/a_0$ is assumed to be isotropic, e_{33}, e_{31} are the piezoelectric coefficients, and a and c are the lattice constants of the strained layer. The relation between the lattice constants in the hexagonal AlGaN system is given by

$$\frac{c-c_0}{c_0}=-2\frac{C_{13}}{C_{33}}\frac{a-a_0}{a_0}, \tag{2}$$

where C_{13} and C_{33} are elastic constants.[26,27] Using Eqs. (1) and (2) the amount of the piezoelectric polarization in the direction of the c axis can be determined by

$$P_{PE}=2\frac{a-a_0}{a_0}\left(e_{31}-e_{33}\frac{C_{13}}{C_{33}}\right). \tag{3}$$

Equation (1) is valid in the linear regime for small strain values. It defines the piezoelectric tensor through the change in polarization induced by variations of the lattice constants a and c only. From a microscopic point of view, a strain parallel or perpendicular to the c axis produces an internal displacement of the metal sublattice with respect to the nitrogen ones, i.e., a variation of the parameter u of the wurtzite structure. The measured piezoelectric polarization is due to the effect of the change of the macroscopic lattice constants and to the associated change in u.

The calculated values of the piezoelectric constants in GaN, InN, and AlN taking both effects into account (see Table I) are up to ten times larger than in GaAs based crystals and the sign is opposite to other III–V compounds.[21] The value of the piezoelectric polarization is increasing with strain and for crystals or epitaxial layers under the same strain from GaN to InN and AlN.

The value of spontaneous polarization is predicted to be very large (comparable to ZnO) and also increasing from GaN to InN and AlN, due to the increasing nonideality of the crystal structure (u increases, c/a decreases, and the difference from the ideal ratio of lattice constants of a closed packed hexagonal structure, $c/a=1.633$, increases as well).[21] The sign of the spontaneous polarization of these group-III nitrides is found to be negative (Table I). The orientation of the spontaneous and piezoelectric polarization is defined assuming that the positive direction goes from the metal (cation) to the nearest neighbor nitrogen atom (anion) along the c axis. Since

$$\left(e_{31}-e_{33}\frac{C_{13}}{C_{33}}\right)<0$$

TABLE I. Lattice constants, spontaneous polarization, piezoelectric, and dielectric constants of AlN, GaN, InN, and BN.

Wurtzite	AlN	GaN	InN	BN
a_0(Å)	3.112	3.189	3.54	2.534[e]
c_0(Å)	4.982	5.185	5.705	4.191[e]
c_0/a_0	1.601	1.627	1.612	1.654[e]
	1.619[a]	1.634[a]	1.627[a]	⋯
u	0.380[a]	0.376[a]	0.377[a]	0.374[e]
P_{SP}(C/m^2)	−0.081[a]	−0.029[a]	−0.032[a]	⋯
e_{33}	1.46[a]	0.73[a]	0.97[a]	⋯
(C/m^2)	1.55[b]	1[c]	⋯	⋯
		0.65[d]	⋯	⋯
	1.29[e]	0.63[e]	⋯	−0.85[e]
e_{31}	−0.60[a]	−0.49[a]	−0.57[a]	⋯
(C/m^2)	−0.58[b]	−0.36[c]	⋯	⋯
		−0.33[d]	⋯	⋯
	−0.38[e]	−0.32[e]	⋯	0.27[e]
e_{15}	−0.48[b]	−0.3[c]	⋯	⋯
(C/m^2)		−0.33[d]	⋯	⋯
ϵ_{11}	9.0[b]	9.5[f]	⋯	⋯
ϵ_{33}	10.7[b]	10.4[f]	14.6[g]	⋯

[a]Reference 21.
[b]Reference 29.
[c]Reference 28.
[d]Reference 32.
[e]References 30 and 31.
[f]Reference 33.
[g]Reference 34.

is valid for AlGaN over the whole range of compositions, from Eq. (3) it follows that the piezoelectric polarization is negative for tensile and positive for compressive strained AlGaN barriers, respectively. As a consequence, the orientation of the piezoelectric and spontaneous polarization is parallel in the case of tensile strain, and antiparallel in the case of compressively strained AlGaN layers. Here we will focus on heterostructures where the AlGaN barriers are always grown on GaN buffer layers and are therefore under tensile strain. In this special case the piezoelectric and the spontaneous polarization point in the same direction and the value of the total polarization is the sum of the piezoelectric and spontaneous polarization

$$P=P_{PE}+P_{SP}. \tag{4}$$

Because the value of the piezoelectric constants and spontaneous polarization increase from GaN to AlN, the total polarization of a strained (or even unstrained) AlGaN layer is larger than that of a relaxed GaN buffer layer [$|P(\text{AlGaN})|\geqslant|P(\text{GaN})|$]. As a consequence of our definition, the negative spontaneous polarization of GaN and AlGaN, as well as the negative piezoelectric polarization of an AlGaN layer under tensile strain, point from the nitrogen towards the nearest neighbor Ga (or the Al atom) along the c axis. As a consequence, the total polarization of both layers is directed towards the c-Al_2O_3 substrate for the Ga-face and towards the surface for the N-face polarity crystals (Fig. 1).

Associated with a gradient of polarization in space is a polarization induced charge density given by

$$\rho_p=-\nabla P. \tag{5a}$$

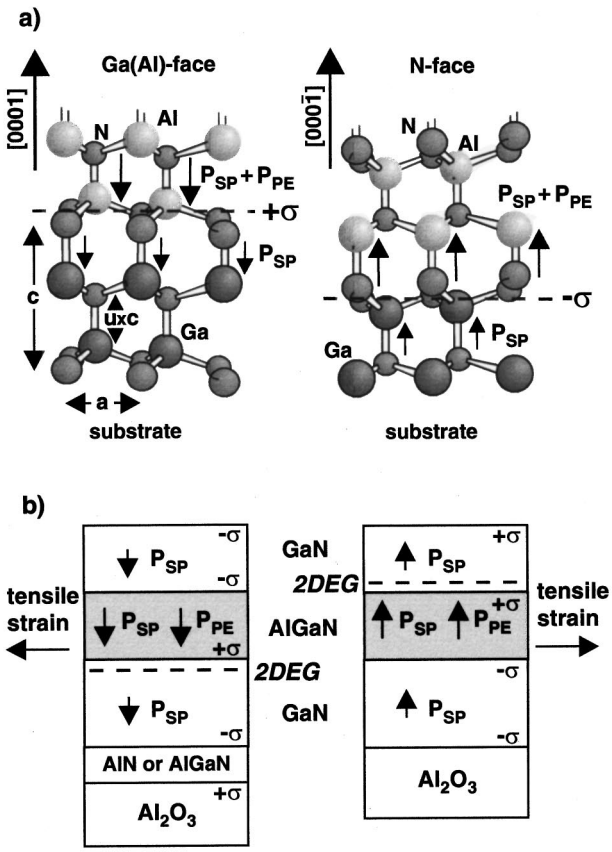

FIG. 1. (a) Crystal structure, polarization induced bound sheet charge, piezoelectric and spontaneous polarization, of pseudomorphic AlN/GaN heterostructures with Ga(Al)-face or N-face polarity. (b) Spontaneous polarization, piezoelectric polarization bound interface charges, and 2DEGs in pseudomorphic GaN/AlGaN/GaN heterostructures with Ga-face or N-face polarity. In Ga-face heterostructures the 2DEG is located close to the lower AlGaN/GaN interface, in N-face heterostructures close to the upper GaN/AlGaN interface.

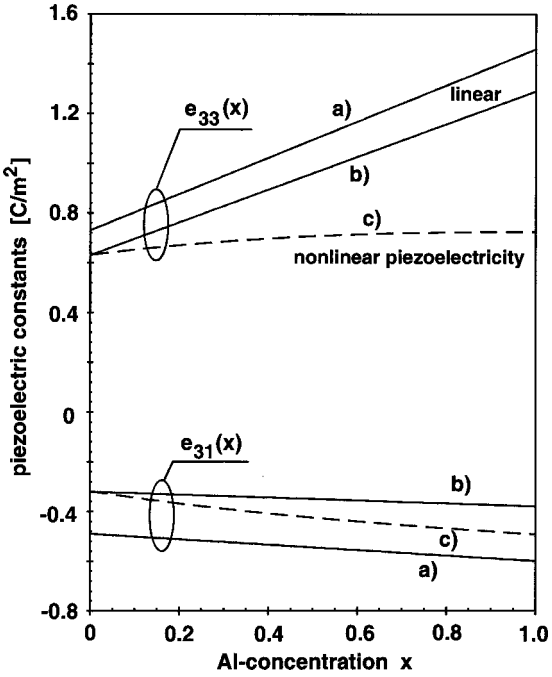

FIG. 2. Piezoelectric constants of AlGaN determined by linear interpolation between the constants of GaN and AlN from different sets of data present in the literature: (a) Ref. 21, (b) Ref. 30, and (c) Ref. 31. The dashed lines show the piezoelectric constants of a pseudomorphic AlGaN layer grown on GaN vs alloy composition calculated by taking strain induced nonlinear effects as predicted by Shimada *et al.* into account.

In analogy, at an abrupt interface of a top/bottom layer heterostructure (AlGaN/GaN or GaN/AlGaN), the polarization can decrease or increase within a bilayer, causing a fixed polarization charge density defined by

$$\begin{aligned}\sigma(P_{\mathrm{SP}}+P_{\mathrm{PE}}) &= P(\mathrm{bottom})-P(\mathrm{top})\\ &= \{P_{\mathrm{SP}}(\mathrm{bottom})+P_{\mathrm{PE}}(\mathrm{bottom})\}\\ &\quad -\{P_{\mathrm{SP}}(\mathrm{top})+P_{\mathrm{PE}}(\mathrm{top})\}\\ &= \{P_{\mathrm{PE}}(\mathrm{bottom})-P_{\mathrm{PE}}(\mathrm{top})\}\\ &\quad +\{P_{\mathrm{SP}}(\mathrm{bottom})-P_{\mathrm{SP}}(\mathrm{top})\}\\ &= \sigma(P_{\mathrm{PE}})+\sigma(P_{\mathrm{SP}}). \qquad (5b)\end{aligned}$$

If the polarization induced charge density is positive $(+\sigma)$, free electrons will tend to compensate the polarization induced charge resulting in the formation of a 2DEG with a sheet carrier concentration n_S, assuming that the triangular quantum well at the AlGaN/GaN interface will drop below the Fermi level E_F. In analogy, a negative sheet charge density $(-\sigma)$ can cause an accumulation of holes at the interface if the valence band edge of the AlGaN/GaN heterostructure crosses the Fermi level. From Eqs. (3), (4), and (5), the polarization induced sheet charge is found to be positive for AlGaN on top of GaN with Ga(Al)-face polarity and GaN on top of AlGaN with N-face polarity. Therefore, the formation of 2DEGs has to be expected at the lower AlGaN/GaN and upper GaN/AlGaN interfaces for Ga- and N-face GaN/AlGaN/GaN heterostructures, respectively (Fig. 1).

O'Clock and Duffy[28] and Tsubouchi[29] determined piezoelectric constants of GaN and AlN by measuring the electromechanical coupling coefficients of thin epitaxial layers grown on sapphire. In addition, piezoelectric constants of GaN, InN, AlN, or BN crystals have been calculated by Bernardini *et al.*[21] and Shimada *et al.*[30] using the Berry phase approach to polarization in solids. The calculated and measured results for GaN and AlN of interest here are in good agreement for e_{33}(AlN) and e_{31}(GaN), but the values of e_{31}(AlN) and e_{33}(GaN) determined experimentally[28,29] or calculated by different groups[21,30] differ by approximately 30%. Furthermore, a large decrease in e_{33} and e_{31} of GaN and AlN with increasing tensile strain was predicted by Shimada *et al.*[31] The changes in e_{33} and e_{31} with strain are attributed to the fact that the piezoelectric constants are significantly influenced by the internal strain component (changes in u) and depend on the structural parameter of the unit cell (changing with the lattice constants), which leads to a nonlinear piezoelectric polarization at higher strains in pseudomorphic $Al_xGa_{1-x}N$/GaN heterostructures.

In order to determine the polarization induced sheet charge located at an AlGaN/GaN interface, the piezoelectric constants of $Al_xGa_{1-x}N$ were linearly interpolated by:

$$e_{ij}(x)=[e_{ij}(\mathrm{AlN})-e_{ij}(\mathrm{GaN})]x+e_{ij}(\mathrm{GaN}). \qquad (6)$$

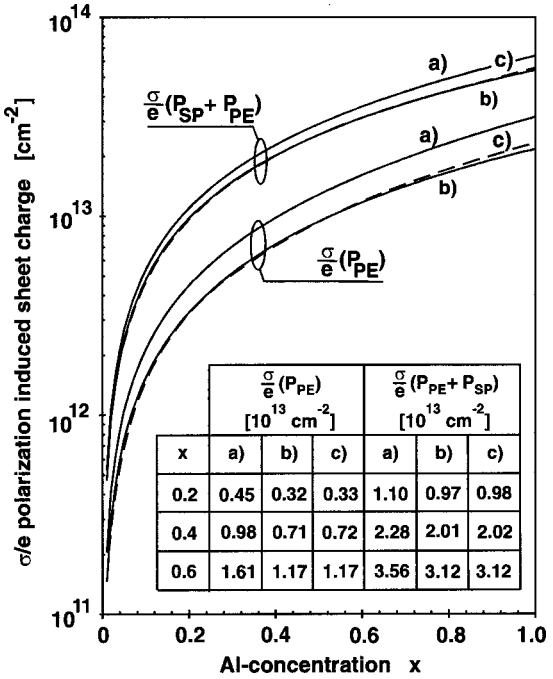

FIG. 3. Bound piezoelectric $\sigma/e(P_{PE})$ and total polarization $\sigma/e(P_{SP}+P_{PE})$ induced sheet charge of pseudomorphic AlGaN/GaN heterostructures vs alloy composition. The sheet charges were calculated by using the piezoelectric constants shown in Fig. 2 (a) Bernardini *et al.* (see Ref. 21), (b) Shimada *et al.* (see Ref. 30), (c) including nonlinear effects (see Ref. 31)) and the spontaneous polarization predicted by Bernardini *et al.* (see Ref. 21). The insert enables a comparision of the calculated sheet charges for alloy compositions of $x=0.2$, 0.4, and 0.6 using the constants of the authors mentioned above.

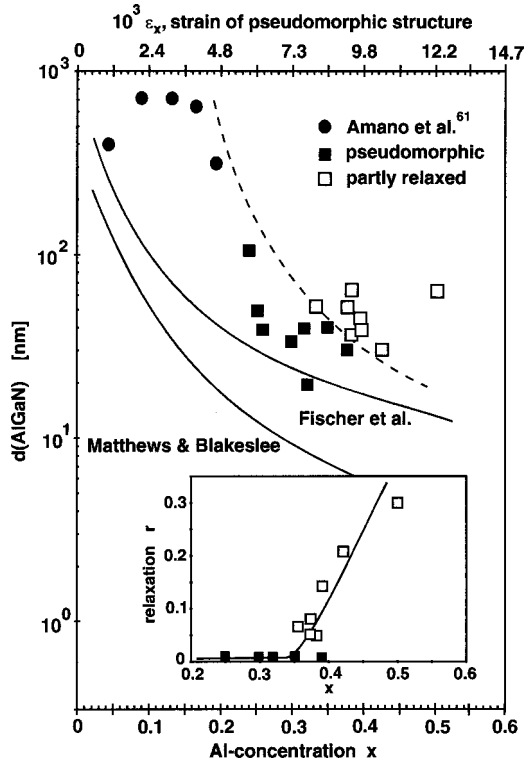

FIG. 4. Critical thickness of AlGaN grown on relaxed GaN calculated using the model of Matthews and Blakeslee (see Ref. 35) or Fischer *et al.* (see Ref. 36) (solid curves) vs Al concentration x (lower horizontal scale), or strain of pseudomorphic grown heterostructures ϵ_x (upper scale). AlGaN layers with different thicknesses and alloy compositions grown pseudomorphically on GaN by MOCVD and PIMBE are marked by black symbols. Partially relaxed AlGaN layers (white symbols) are separated from pseudomorphic heterostructures by a dashed line. The insert shows the degree of relaxation $r(x)$ measured by HRXRD vs alloy compositions for AlGaN barriers with a thickness of about 300 Å.

To compare the value of the polarization induced charge evaluated from different sets of piezoelectric constants, we used the results obtained by Bernardini *et al.*[21] and Shimada *et al.*[30] summarized in Table I. To calculate the influence of nonlinearity on σ, the piezoelectric constants were taken from Ref. 31. In general, the values of the piezoelectric constants $|e_{33}(x)|$ and $|e_{31}(x)|$ are increasing with increasing Al concentration. The constants interpolated from the results of Shimada *et al.* are about 15% and 35% smaller for $|e_{33}(x)|$ and $|e_{31}(x)|$, respectively, than the values interpolated from the data of Bernardini *et al.* Taking into account the decrease of piezoelectric constants with increasing strain for $Al_xGa_{1-x}N$ layers grown pseudomorphically on GaN, the change of $|e_{33}(x)|$ becomes negligible and the increase of $|e_{31}(x)|$ turns out to be more significant if the Al concentration of the barrier is increased (Fig. 2).

To calculate the amount of the polarization induced sheet charge density, σ/e ($e=1.602\times10^{-19}$ C), bound at the interfaces of pseudomorphically grown $Al_xGa_{1-x}N$/GaN and GaN/$Al_xGa_{1-x}N$ structures, we use the following set of linear interpolations between the physical properties of GaN and AlN:[16]

lattice constants:

$$a_0(x)=(-0.077x+3.189)10^{-10}\ \text{m}, \tag{7}$$

$$c_0(x)=(-0.203x+5.189)10^{-10}\ \text{m}, \tag{8}$$

elastic constants:

$$C_{13}(x)=(5x+103)\text{GPa}, \tag{9}$$

$$C_{33}(x)=(-32x+405)\text{GPa}, \tag{10}$$

and

spontaneous polarization:

$$P_{SP}(x)=(-0.052x-0.029)\frac{\text{C}}{\text{m}^2}. \tag{11}$$

The value of the bound sheet charge caused by the piezoelectric polarization of the AlGaN under tensile strain, $\sigma/e(P_{PE})$, increases more than linearly with increasing Al concentration. To give an example, $\sigma/e(P_{PE})$ increases from 0.32×10^{13} to $0.71\times10^{13}\,\text{cm}^{-2}$ using the constants of Shimada *et al.*[30] [Fig. 3(b)] or from 0.45×10^{13} to $0.98\times10^{13}\,\text{cm}^{-2}$ using the constants of Bernardini *et al.*[21] [Fig. 3(a)] if the alloy composition is changed from $x=0.2$ to 0.4. Surprisingly, by taking into account the nonlinearity of the piezoelectric constants and in turn of the piezoelectric polarization, the sheet charge is only changed by about 2% [Fig. 3(c)]. This indicates that the influence of nonlinear effects caused by strain on the polarization induced sheet charge is negligible. The value of the total polarization induced sheet charge, $\sigma/e(P_{SP}+P_{PE})$, is about twice as high as the piezoelectric polarization induced sheet charge caused by the sig-

nificant change of spontaneous polarization at the AlGaN/GaN interface. By increasing the alloy composition of the AlGaN barrier from $x=0.2$ to 0.4 the total sheet charge increases from 0.97×10^{13} to $2.01\times10^{13}\,\mathrm{cm}^{-2}$ or 1.1×10^{13} to $2.28\times10^{13}\,\mathrm{cm}^{-2}$ using again the piezoelectric constants of Shimada or Bernardini, respectively. The uncertainty in the calculated total polarization sheet charge caused by the differences in the piezoelectric constants from these two references is below 15% over the entire range of alloy compositions.

Up to now we have determined the piezoelectric and total polarization sheet charge assuming that the AlGaN barrier is grown pseudomorphically on GaN. Calculations of the critical thickness of hexagonal AlGaN grown on relaxed GaN applying the model invented by Matthews and Blakeslee[35] (or Fischer *et al.*[36]) show that for a typical barrier thickness of about 300 Å, strain relaxation and therefore reduction in piezoelectric polarization has to be expected for alloy compositions above $x=0.14$ (or 0.25). The critical thicknesses calculated from the models mentioned above for different alloy compositions are shown in Fig. 4 (solid lines). In order to measure the alloy composition and relaxation of the barriers, the lattice constants $a(x)$ and $c(x)$ of GaN and AlGaN were determined by high resolution x-ray diffraction (HRXRD). Reciprocal space maps of the (00.2) and (20.5) reflections of AlGaN/GaN heterostructures with barrier thicknesses between 200 and 1000 Å and alloy compositions up to $x=0.5$ were investigated.[16,25] The Al concentration x and degree of relaxation $r(x)$ were calculated by[37]

$$x=-\frac{a(x)c(x)\{1+\nu\}-a(x)c_0(\mathrm{GaN})-a_0(\mathrm{GaN})c(x)\nu}{a(x)c_0(\mathrm{GaN})-a(x)c_0(\mathrm{AlN})-a_0(\mathrm{AlN})c(x)\nu+a_0(\mathrm{GaN})c(x)\nu}, \tag{12}$$

and

$$r(x)=\frac{a(x)-a(\mathrm{GaN})}{a_0(x)-a(\mathrm{GaN})}, \tag{13}$$

where $\nu=2C_{13}(x)/C_{33}(x)$ and the change of c/a with alloy composition was neglected. The onset in macroscopic strain relaxation was detected for barrier thicknesses well above the calculated critical thicknesses over a broad range of alloy compositions (see dashed line in Fig. 4). For barrier thicknesses of 300 ± 50 Å macroscopic strain relaxation was first observed for alloy compositions of $x=0.38\pm0.03$. The degree of relaxation increased linearly with increasing Al concentration for higher values of x (inset of Fig. 4). To calculate the reduction of piezoelectric polarization and the polarization induced sheet charge due to strain relaxation, the measured degree of relaxation was approximated by

$$r(x)=\begin{cases}0 & 0\leqslant x<0.38\\ 3.5x-1.33 & 0.38\leqslant x\leqslant 0.67\\ 1 & 0.67<x\leqslant 1\end{cases}, \quad \text{for } d(\mathrm{AlGaN})\approx 300\ \text{Å}. \tag{14}$$

The piezoelectric polarization for partially relaxed barriers can be determined by using the measured lattice constants [Eq. (2)] or from the measured degree of relaxation by

$$P_{\mathrm{PE}}(x)=2\{r(x)-1\}\left\{\frac{a_0(x)-a(\mathrm{GaN})}{a_0(x)}\right\}\times\left\{e_{31}(x)-e_{33}(x)\frac{C_{13}(x)}{C_{33}(x)}\right\}. \tag{15}$$

For a barrier with a fixed alloy composition, the piezoelectric polarization and therefore the corresponding sheet charge, $\sigma/e(P_{\mathrm{PE}})$, decreases linearly with increasing degree of relaxation. As a consequence, the maximum piezoelectric polarization induced sheet charge, which can be reached by increasing the Al concentration of the barrier in HEMTs, is limited by strain relaxation. The bound sheet charge induced by only piezoelectric polarization of AlGaN barriers with different degrees of relaxation is shown in Fig. 5 (dashed lines). The maximum sheet charge caused by piezoelectric polarization of a strained 300 Å thick barrier was calculated by using the measured degree of relaxation $r(x)$ to be $0.92\times10^{13}\,\mathrm{cm}^{-2}$ reached at $x=0.38$ [see the solid curve labeled by $r(x)$ in Fig. 5].

The total polarization as well as the corresponding sheet charge calculated by taking the difference in spontaneous polarization of GaN and AlGaN into account, decreases also linearly with increasing degree of relaxation. For a barrier with $x=0.4$ the total sheet charge, $\sigma/e(P_{\mathrm{SP}}+P_{\mathrm{PE}})$, is predicted to decrease from 2.28×10^{13} to $1.30\times10^{13}\,\mathrm{cm}^{-2}$ if the AlGaN becomes completely relaxed. The calculated total bound sheet charge is shown in Fig. 6 versus Al concentration and different degrees of relaxation of the barrier. It is important to note that because of the difference in spontaneous polarization of GaN and AlGaN layers, the sheet charge does not drop to zero for an unstrained barrier. For barriers where the degree of relaxation can be described by $r(x)$, the

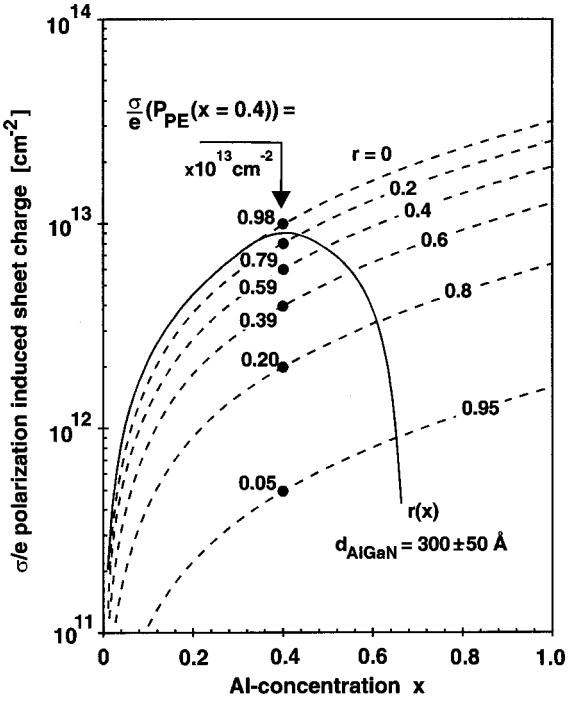

FIG. 5. Calculated piezoelectric polarization induced sheet charge $\sigma/e(P_{PE})$ for pseudomorphically grown AlGaN/GaN heterostructures $r=0$, and barriers with different degrees of relaxation $r=0.2$, 0.4,..., vs Al concentration of the top layer (dashed lines). The piezoelectric polarization of the AlGaN layer was calculated by Eq. (15), and the bound sheet charges $\sigma(P_{PE})$ by Eq. (5b) neglecting spontaneous polarization. The solid line represents $\sigma/e(P_{PE})$ for AlGaN barriers with a thickness of about 300 Å by talking into account the measured degrees of relaxation $r(x)$ [see Eq. (14)].

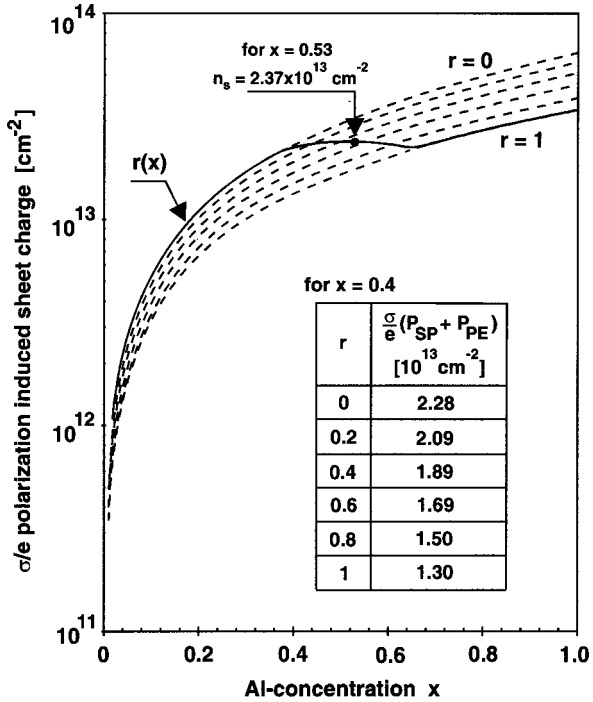

FIG. 6. Calculated piezoelectric and spontaneous polarization induced sheet charge, $\sigma/e(P_{SP}+P_{PE})$ for pseudomorphically grown AlGaN/GaN heterostructures $r=0$, and barriers with different degrees of relaxation $r=0.2$, 0.4,..., vs Al concentration of the top layer (dashed lines). The spontaneous and piezoelectric polarization of the AlGaN layer was calculated by Eqs. (11) and (15), the bound sheet charges $\sigma(P_{SP}+P_{PE})$ by Eq. (5b). The solid line represents $\sigma/e(P_{SP}+P_{PE})$ for AlGaN barriers with a thickness of about 300 Å by talking into account the measured degrees of relaxation $r(x)$ [see Eq. (14)]. The inset shows the calculated sheet charges for different degrees of relaxation of an $Al_{0.4}Ga_{0.6}N$/GaN heterostructure.

polarization induced sheet charge is found to reach 2.37 $\times 10^{13}\,\mathrm{cm}^{-2}$ at an alloy composition of 53%. For Al concentrations higher than 72% the sheet charge is further increased up to $3.24\times 10^{13}\,\mathrm{cm}^{-2}$, even if the barrier is completely relaxed, caused by the increase of spontaneous polarization of the AlGaN layer with increasing Al concentration.

With a theoretical understanding of the polarization induced charge we now wish to predict the sheet carrier concentration of a 2DEG and its dependence on alloy composition for strained AlGaN/GaN based heterostructures.

IV. SHEET CARRIER CONCENTRATIONS OF TWO DIMENSIONAL ELECTRON GASES

Free electrons tend to compensate a positive polarization induced sheet charge which is bound at the lower AlGaN/GaN interface for Ga(Al)-face or at the upper GaN/AlGaN interface for N-face GaN/AlGaN/GaN HEMT structures [Fig. 1(b)]. The value of the total polarization induced sheet charge is the same in heterostructures of different polarities for a given Al concentration and strain of the barrier. For undoped Ga-face AlGaN/GaN or GaN/AlGaN/GaN HEMT structures, the sheet electron concentration $n_S(x)$ can be calculated by using the total bound sheet charge $\sigma(x)$ and the following equations:[17,38]

$$n_S(x)=\frac{\sigma(x)}{e}-\left(\frac{\epsilon_0\epsilon(x)}{d_{\mathrm{AlGaN}}e^2}\right)[e\phi_b(x)+E_F(x)-\Delta E_C(x)], \tag{16a}$$

or

$$n_S(x)=\left\{1+\frac{\epsilon(x)}{\epsilon(0)}\frac{d_{\mathrm{GaN}}}{d_{\mathrm{AlGaN}}}\right\}^{-1}\left\{\frac{\sigma(x)}{e}-\left(\frac{\epsilon_0\epsilon(x)}{d_{\mathrm{AlGaN}}e^2}\right)\times[e\phi_b^{\mathrm{eff}}(x)+E_F(x)-\Delta E_C]\right\}, \tag{16b}$$

respectively. $\epsilon(x)$ is the relative dielectric constant of $Al_xGa_{1-x}N$, d_{AlGaN} and d_{GaN} are the thicknesses of the barrier and the cap layer, $e\Phi_b(x)$ [and $e\Phi_b^{\mathrm{eff}}(x)$] are the (effective) Schottky barriers of the gate contact on top of AlGaN (or GaN/AlGaN),[39] $E_F(x)$ is the Fermi level with respect to the GaN conduction-band-edge energy, and ΔE_C is the conduction band offset at the AlGaN/GaN interface where a 2DEG forms. For undoped HEMT structures and assuming that the background concentration of free carriers can be neglected ($N_d<10^{16}\,\mathrm{cm}^{-3}$), it is found from Eq. (16) that the value of the sheet carrier concentration is dominated by the total polarization induced sheet charge which can be controlled by the alloy composition of the barrier. The sheet carrier concentration will be reduced with increasing height of the Schottky barrier and decreasing thickness of the barrier. The effect on the calculated sheet carrier concentration due to the uncertainty in the dielectric constant and conduction band offset is found to be negligible.

To enable the determination of the sheet carrier concentration and carrier distribution profile in doped and undoped

HEMT structures, including spontaneous and piezoelectric polarization induced bound sheet charges, we have used a one dimensional Schrödinger–Poisson solver.[40] To incorporate the effects of spontaneous and piezoelectric polarization into the program, thin layers (≈6 Å) of charge are added to the heterostructure interfaces equivalent to the bound sheet charge density σ/e. It is also necessary to specify the boundary conditions at the surface and substrate interfaces. In our structures we assumed a Ni Schottky barrier contact at the surface, pinning the conduction band. At the interface, towards the substrate, the Fermi level was set to one half of the band gap of GaN. By changing the value of the conduction band level close to the substrate it turned out that this boundary condition has very little impact on the sheet carrier concentration of the 2DEG for buffer thicknesses above 1 μm. In agreement with the measured electron concentrations the background free carrier concentration in our calculation was assumed to be $10^{14}\,\mathrm{cm}^{-3}$ in the entire heterostructure. We used the following linear interpolations for the physical properties of $Al_xGa_{1-x}N$ in our calculations:

dielectric constant:

$$\epsilon(x) = -0.3x + 10.4, \tag{17}$$

Ni Schottky barrier:[41]

$$e\phi_b = (1.3x + 0.84)\,\mathrm{eV}, \tag{18}$$

band offset:[42,43]

$$\Delta E_C = 0.7[E_g(x) - E_g(0)], \tag{19}$$

where the band gap of $Al_xGa_{1-x}N$ is measured to be[44]

$$E_g(x) = xE_g(\mathrm{AlN}) + (1-x)E_g(\mathrm{GaN}) - x(1-x)1.0\ \mathrm{eV}, \tag{20}$$

$$= x6.13\ \mathrm{eV} + (1-x)3.42\ \mathrm{eV} - x(1-x)1.0\ \mathrm{eV}, \tag{21}$$

and an effective electron mass of $m^* = 0.228$ in GaN is determined.[45] We find very good agreement between the sheet carrier concentrations calculated for undoped HEMTs by Eq. (16) and the self-consistent solution of our Schrödinger–Poisson solver. The barrier layer of the doped HEMT consisted of an undoped spacer layer (30 Å), a doped region (100 Å) with a silicon concentration of $1\times10^{19}\,\mathrm{cm}^{-3}$, and an undoped top region (60 Å). The sheet carrier concentration of the undoped and doped heterostructures were calculated to be 1.46×10^{13} and $1.60\times10^{13}\,\mathrm{cm}^{-2}$, respectively. The average distance between the 2DEGs and the $Al_{0.33}Ga_{0.67}N$/GaN interface was determined to be 17 Å for the undoped and 10 Å for the doped HEMT structure. The contribution of the sheet carrier concentrations located inside the barrier was calculated to be 0.18×10^{13} and $0.31\times10^{12}\,\mathrm{cm}^{-3}$ for the undoped and doped structure, respectively, meaning that higher gate leakage currents have to be expected for the doped HEMTs. The experiments to determine the sheet carrier concentrations of the above structures were carried out by Hall effect and $C-V$ profiling measurements.[16] Examples of the measured and calculated electron distributions in undoped ($d_{\mathrm{AlGaN}}=300$ Å) and doped ($d_{\mathrm{AlGaN}}=190$ Å) Ga-face $Al_{0.33}Ga_{0.67}N$/GaN heterostructures are shown in Fig. 7. The sheet carrier concentrations of the undoped and doped structures measured by $C-V$ profiling

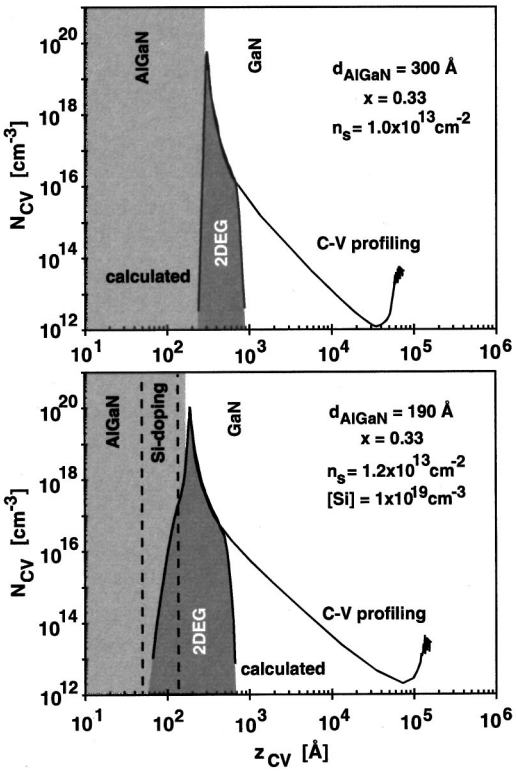

FIG. 7. Measured and calculated sheet carrier distributions of 2DEGs located close to the interface of pseudomorphically grown Ga-face $Al_{0.33}Ga_{0.67}N$/GaN HEMTs. A sheet carrier concentration of $1\times10^{13}\,\mathrm{cm}^{-2}$ was determined by $C-V$ profiling for an undoped barrier with a thickness of 300 Å. For a 190 Å thick doped barrier with a silicon concentration of $1\times10^{19}\,\mathrm{cm}^{-3}$ over a depth of 100 Å (spacer layer 30 Å) a sheet carrier concentration of $1.2\times10^{13}\,\mathrm{cm}^{-2}$ was observed at room temperature.

were found to be 1.0×10^{13} and $1.2\times10^{13}\,\mathrm{cm}^{-2}$, which is $4\times10^{12}\,\mathrm{cm}^{-2}$ less than the calculated sheet carrier concentrations. The background concentration of free carriers in the barrier and buffer layer was measured to be below 10^{17} and $10^{14}\,\mathrm{cm}^{-3}$ ($n_S<10^{12}\,\mathrm{cm}^{-2}$), respectively.

To enable a more detailed comparison of calculated and measured data, we determined the sheet carrier concentrations of Ga-face AlGaN/GaN heterostructures with undoped and doped (as described above) barriers with thicknesses of about 200 Å and alloy compositions up to $x=0.6$. Sheet carrier concentrations caused by only piezoelectric $n_S(P_{\mathrm{PE}})$, as well as by piezoelectric and spontaneous polarization $n_S(P_{\mathrm{PE}}+P_{\mathrm{SP}})$, were calculated for pseudomorphic ($r=0$) and partialy relaxed barriers [$r=r(x)$]. The results are summarized in Table II and are shown in Fig. 8. By taking into account only the piezoelectric polarization of pseudomorphically grown barriers, the sheet carrier concentration increases more than linearly from 0.19×10^{13} to $1.27\times10^{13}\,\mathrm{cm}^{-2}$ if the Al concentration is increased from $x=0.2$ to 0.6. For partially relaxed barriers a maximum sheet carrier concentration of $0.64\times10^{13}\,\mathrm{cm}^{-2}$ is reached at $x=0.38$. It should be mentioned that for thinner barrier strain relaxation will probably occur at higher Al concentrations and a further increase of the piezoelectric polarization induced sheet charge has to be expected [see dashed line of $n_S(P_{\mathrm{PE}})$ in Fig. 8].[46,47] The predicted sheet carrier concentration induced by the total po-

TABLE II. Calculated sheet carrier concentrations induced by only piezoelectric or spontaneous and piezoelectric polarization in undoped and doped $Al_xGa_{1-x}N$/GaN HEMT structures. The sheet carrier concentrations are given for different alloy compositions, $x=0.1, 0.2,..., 0.6$ of pseudomorphically, $r=0$, and partialy relaxed, $r=r(x)$, grown barriers with a thickness of 200 Å.

	Undoped				Doped	
$T=300$ K	$n_S(P_{PE})$ (10^{13} cm^{-2})		$n_S(P_{PE}+P_{SP})$ (10^{13} cm^{-2})		$n_S(P_{PE}+P_{SP})$ (10^{13} cm^{-2})	
x	$r=0$	$r=r(x)$	$r=0$	$r=r(x)$	$r=0$	$r=r(x)$
0.1	<0.1	<0.1	0.263	0.263	0.527	0.527
0.2	0.198	0.198	0.766	0.766	1.042	1.042
0.3	0.437	0.437	1.289	1.289	1.595	1.595
0.4	0.694	0.634	1.831	1.771	2.184	2.036
0.5	0.972	0.499	2.394	1.921	2.818	2.261
0.6	1.270	0.184	2.979	1.892	3.490	2.217

larization sheet charge is more than twice as high as the sheet carrier concentration induced just by the piezoelectric effect. The sheet carrier concentration in undoped HEMTs increases up to 2.98×10^{13} cm^{-2} for $r=0$ and $x=0.6$. For partially relaxed barriers a maximum sheet carrier concentration of 1.9×10^{13} cm^{-2} can be reached for the same alloy composition. For doped HEMTs a maximum sheet carrier concentration of 1.04×10^{13} cm^{-2} is calculated for $x=0.2$ increasing to 3.5×10^{13} cm^{-2} for $x=0.6$.

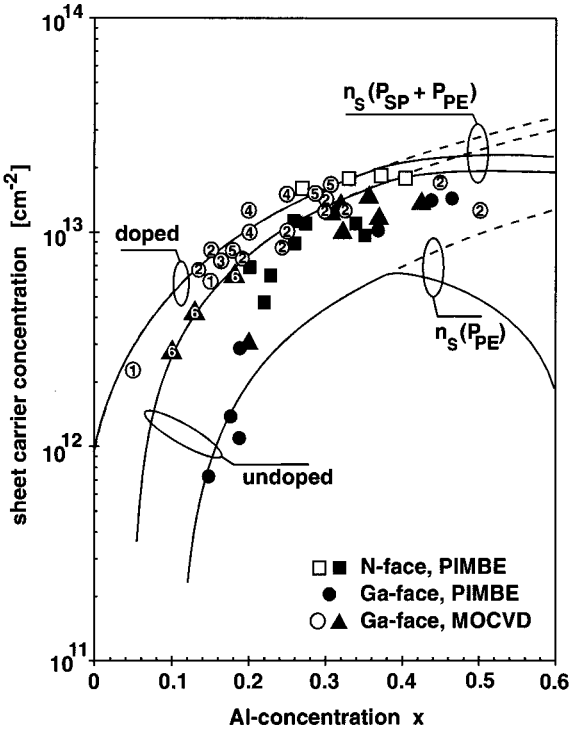

FIG. 8. Calculated maximum sheet carrier concentrations $n_S(P_{SP}+P_{PE})$ for pseudomorphic (dashed lines) and partialy relaxed [relaxation described by Eq. (14), solid lines] Ga-face $Al_xGa_{1-x}N$/GaN HEMT structures with a barrier thickness of 200 Å. The upper two curves are showing $n_S(P_{SP}+P_{PE})$ for doped and undoped barriers, respectively. The maximum sheet carrier concentration induced by only piezoelectric polarization of the barrier $n_S(P_{PE})$ is shown for comparison (lower curve). Black symbols are the sheet carrier concentrations determined by Hall effect measurements ($T=300$ K) for undoped AlGaN/GaN and GaN/AlGaN/GaN heterostructures. White symbols are measured and published data for doped HEMTs: (1) Ref. 45, (2) Refs. 48–50, (3) Ref. 51, (4) Refs. 52–53, and (5) Refs. 54 and 55. In addition sheet carrier concentrations of undoped HEMTs measured by Shubnikov–de Haas oscillations are presented, (6) Ref. 56.

By comparison of the calculated and measured sheet carrier concentrations for doped and undoped HEMTs with different alloy compositions shown in Fig. 8 the following conclusions can be extracted:

(i) Since the calculated sheet densities can be considered as an upper bound, it is evident from the fact that the measured sheet carrier concentrations for undoped HEMTs are higher than the calculated sheet carrier concentrations induced by only piezoelectric polarization $n_S(\mathrm{PE})$ that spontaneous polarization is real and has to be taken into account in the determination of the total sheet charges and sheet carrier concentrations.

(ii) We find a good agreement between the calculated and experimentally determined *highest* sheet carrier concentrations, $n_S(P_{SP}+P_{PE})$, for undoped and doped HEMTs. The *highest* sheet carrier concentrations measured over a broad range of alloy compositions ($0.05\leqslant x\leqslant 0.45$) as well as published data[45,48–56] agree within $\pm20\%$ with the prediction of our theoretical model. As a consequence the predicted difference in total polarization between GaN and AlGaN must be valid with the same accuracy.

(iii) Even with heavy doping of the barrier the measured and calculated differences in the highest sheet carrier concentrations between doped and undoped AlGaN/GaN heterostructures with the same Al concentration and strain is below 15%. This observation demonstrates that the formation of 2DEGs in HEMT structures is dominated by polarization induced effects.

The observed scattering of the measured sheet carrier concentrations of heterostructures with similar barrier thicknesses and alloy compositions is unexpected and well above the error of our experiments. Beside strain relaxation or screening of polarization induced electric fields by free carriers the sheet carrier concentration of the 2DEGs might be reduced by:

(i) roughness of the AlGaN/GaN interface,
(ii) the gradient in alloy composition close to the AlGaN/GaN interface,
(iii) the presence of N- and Ga-face polarity beside each other, and
(iv) electron traps due to dislocations or surface states.

Interface roughness and a gradient in Al concentration close to the interface smears out the bound polarization induced charge over a larger distance. By transmission electron microscopy (TEM) and elastic recoil detection analysis[37] of MOCVD and PIMBE grown $Al_{0.3}Ga_{0.7}N$/GaN HEMTs, the interface roughness and width in which the Al concentration changed was determined to be between 20 and 50 Å. Assuming that the polarization induced charge is homogeneously distributed over a width of 50 Å, the sheet carrier concentration decreases from 1.45×10^{13} calculated for an abrupt interface to 1.43×10^{13} cm^{-2}. Even if the sheet charge is distributed over a width of up to 200 Å, the calculated sheet

carrier concentration is only decreased to $1.38\times10^{13}\,\mathrm{cm}^{-2}$. This demonstrates that the effects of interface roughness and alloy composition gradients on the sheet carrier concentration is negligible in our heterostructures. It should be mentioned that according to the calculations, interface roughness, and composition gradients at the AlGaN/GaN interface will increase the amount of free carriers in the barrier. Furthermore both effects will cause a strong scattering of electrons resulting in a reduction in the 2DEG mobility, mainly because of the small average distance between the 2DEG and the interface.[8,16] These will degrade the performance of HEMTs by reducing the source drain current and increasing the gate leakage current.

Strong reduction of polarization effects can be caused by the presence of Ga- and N-face polarity in one sample. Heterostructures grown on GaN buffer layers with mixed polarities will have polarization induced sheet charges with different signs at the same interface. These charges will tend to compensate one another, leading to a strong reduction of sheet carrier concentration. These effects can be ruled out for our optimized heterostructures. No evidence of mixed polarities was observed by the x-ray standing wave method or corresponding inversion domain boundaries were found by TEM.[23]

The dislocation density for our HEMTs grown by MOCVD and PIMBE was found to be between 5×10^{8} and $5\times10^{9}\,\mathrm{cm}^{-2}$ by AFM and TEM. Recent charge state calculations for AlN and GaN predict that threading dislocations produce defect levels in the band gap. In agreement with experimental studies, edge dislocations are calculated to be negatively charged by trapping free electrons in *n*-type GaN. The amount of charge accumulation at dislocations can be quantified using the models of Weimann *et al.*[57] or Leung *et al.*[58] The reduction of the sheet carrier concentration caused by electron traps due to dislocations in a $Al_{0.3}Ga_{0.7}N$/GaN HEMT can be estimated using the published relationship[57] between free carrier concentration and charge accumulation at dislocations. From the calculated carrier distribution profiles of the 2DEGs, the reduction of sheet carrier concentrations was estimated to be between 5×10^{11} and $5\times10^{12}\,\mathrm{cm}^{-2}$ for the measured range of dislocation densities. This indicates that the scattering of the measured 2DEG sheet carrier concentrations for samples with the same alloy composition and thickness of the barrier can be caused by different dislocation densities. In addition, trapping of electrons due to dislocations could be one explanation for the experimental observation that the predicted increase of sheet carrier concentration with increasing doping concentration of the barrier is up to $4\times10^{12}\,\mathrm{cm}^{-2}$ [for $n(\mathrm{Si})=2\times10^{13}\,\mathrm{cm}^{-2}$] higher than the measured electron sheet density.

Fermi level pinning at a semiconductor surface can result in the formation of a dipole field near the surface. Photoemission and angle resolved photoemission spectroscopy has been used recently to study wurtzite GaN and substantial band bending due to Fermi level pinning at the sample surface has been reported.[59] Dhesi *et al.* found the valence band maximum of a clean *n*-type GaN surface 1.3 eV below E_F, indicating a large upward band bending of 2.1 eV.[60] If similar defect states exist at the surface (or interface) of our AlGaN/GaN HEMT structures, pinning E_F and causing large upward band bending, a reduction of sheet carrier concentration of the 2DEGs might be the result.

V. SUMMARY

In conclusion, we have calculated polarization induced sheet charges bound at AlGaN/GaN interfaces from different sets of piezoelectric constants available in the literature, using linear interpolations between the physical properties of GaN and AlN. Although the differences in the piezoelectric constants was found to be significant, especially when the predicted influence of strain on the piezoelectric polarization was taken into account, the bound polarization induced sheet charge could be calculated over the whole range of compositions with an accuracy of about 20%. The influence of strain induced nonlinear effects on the piezoelectric induced polarization charge was found to be negligible.

For typical AlGaN/GaN HEMT structures ($d_{\mathrm{AlGaN}}\approx300$ Å) macroscopic relaxation of tensile strain was determined by HRXRD for alloy compositions above 38%, limiting the maximum piezoelectric polarization induced charge to $\sigma/e(P_{\mathrm{PE}})=9\times10^{12}\,\mathrm{cm}^{-2}$. The polarization induced sheet carrier concentrations of 2DEGs were calculated by self-consistent solutions of the Schrödinger and Poisson equations and compared with experimental results obtained by $C-V$ profiling and Hall effect measurements. The measured sheet carrier concentrations of undoped and doped HEMT structures were found to be significantly higher than the values calculated taking only piezoelectric effects into account, and thereby demonstrating that spontaneous polarization has to be considered to explain the measured 2DEG densities. We found a good agreement between highest measured and calculated 2DEG sheet carrier concentrations for undoped and doped HEMTs. The scattering and discrepancies between the observed sheet carrier concentrations and the calculated results for undoped AlGaN/GaN heterostructures can be explained by the trapping of carriers due to dislocations and surface states.

ACKNOWLEDGMENTS

O. Ambacher would like to thank the Alexander von Humboldt Stiftung for a Feodor Lynen fellowship, and to acknowledge financial support from the Deutsche Forschungsgemeinschaft (Grant No. Stu 139/2). The work done at Cornell University is supported by the Office of Naval Research under Contract Nos. N00014-96-1-1223 and N00014-95-1-0926 under the direction of Dr. J. Zolper.

[1] O. Ambacher, J. Phys. D **31**, 2653 (1998).
[2] A. Ozgur, W. Kim, Z. Fan, A. Botchkarev, A. Salvador, S. N. Mohammad, B. Sverdlov, and H. Morkoc, Electron. Lett. **31**, 1389 (1995).
[3] M. A. Khan, Q. Chen, M. S. Shur, B. T. McDermott, J. A. Higgins, J. Burm, W. J. Schaff, and L. F. Eastman, IEEE Electron Device Lett. **17**, 584 (1996).
[4] S. C. Binari, J. M. Redwing, G. Kelner, and W. Kruppa, Electron. Lett. **33**, 242 (1997).
[5] R. Gaska, Q. Chen, J. Yang, A. Osinsky, M. A. Khan, and M. S. Shur, IEEE Electron Device Lett. **18**, 492 (1997).
[6] Y. F. Wu, S. Keller, P. Kozodoy, B. P. Keller, P. Parish, D. Kapolnek, S. P. DenBaars, and U. K. Mishra, IEEE Electron Device Lett. **18**, 290 (1997).

[7] R. Dimitrov, L. Wittmer, H. P. Felsl, A. Mitchell, O. Ambacher, and M. Stutzmann, Phys. Status Solidi A **168**, R7 (1998).
[8] R. Oberhuber, G. Zandler, and P. Vogl, Appl. Phys. Lett. **73**, 818 (1998).
[9] Y. Zhang and J. Singh, J. Appl. Phys. **85**, 587 (1999).
[10] M. Shur, *GaAs Devices and Circuits* (Plenum, New York, 1986).
[11] B. E. Foutz, L. F. Eastman, U. V. Bhapkar, and M. S. Shur, Appl. Phys. Lett. **70**, 2849 (1997).
[12] K. K. Chu, J. A. Smart, J. R. Shealy, and L. F. Eastman, IEEE Electron. Device Lett. (in press).
[13] S. T. Sheppard, K. Doverspike, W. L. Pribble, S. T. Allen, J. W. Palmour, L. T. Kehias, and T. J. Jenkins, IEEE Electron Device Lett. **20**, 161 (1999).
[14] W. Q. Chen and S. K. Hark, J. Appl. Phys. **77**, 5747 (1995).
[15] A. Bykhovski, B. L. Gelmont, and M. S. Shur, J. Appl. Phys. **81**, 6332 (1997).
[16] O. Ambacher, J. Smart, J. R. Shealy, N. G. Weimann, K. Chu, M. Murphy, W. J. Schaff, L. F. Eastman, R. Dimitrov, L. Wittmer, M. Stutzmann, W. Rieger, and J. Hilsenbeck, J. Appl. Phys. **85**, 3222 (1999).
[17] P. M. Asbeck, E. T. Yu, S. S. Lau, G. J. Sullivan, J. Van Hove, and J. M. Redwing, Electron. Lett. **33**, 1230 (1997).
[18] E. T. Yu, G. J. Sullivan, P. M. Asbeck, C. D. Wang, D. Qiao, and S. S. Lau, Appl. Phys. Lett. **71**, 2794 (1997).
[19] M. B. Nardelli, K. Rapcewicz, and J. Bernholc, Appl. Phys. Lett. **71**, 3135 (1997).
[20] T. Takeuchi, H. Takeuchi, S. Sota, H. Sakai, H. Amano, and I. Akasaki, Jpn. J. Appl. Phys., Part 2 **36**, L177 (1997).
[21] F. Bernardini, V. Fiorentini, and D. Vanderbilt, Phys. Rev. B **56**, R10024 (1997).
[22] J. A. Smart, A. T. Schremer, N. G. Weimann, O. Ambacher, L. F. Eastman, and J. R. Shealy, Appl. Phys. Lett. **75**, 388 (1999).
[23] A. Kazimirov, G. Scherb, J. Zegenhagen, T.-L. Lee, M. J. Bedzyk, M. K. Kelly, H. Angerer, and O. Ambacher, J. Appl. Phys. **84**, 1703 (1998).
[24] M. J. Murphy, K. Chu, H. Wu, W. Yeo, W. J. Schaff, O. Ambacher, J. Smart, J. R. Shealy, L. F. Eastman, and T. J. Eustis, J. Vac. Sci. Technol. B **17**, 1252 (1999).
[25] R. Dimitrov, A. Mitchell, L. Wittmer, O. Ambacher, and M. Stutzmann, Jpn. J. Appl. Phys. **38**, 4962 (1999).
[26] A. F. Wright, J. Appl. Phys. **82**, 2833 (1997).
[27] C. Deger, E. Born, H. Angerer, O. Ambacher, M. Stutzmann, J. Hornsteiner, E. Riha, and G. Fischerauer, Appl. Phys. Lett. **72**, 2400 (1998).
[28] G. D. O'Clock and M. T. Duffy, Appl. Phys. Lett. **23**, 55 (1973).
[29] K. Tsubouchi, K. Sugai, and N. Mikoshiba, IEEE Ultrason. Symp. **1**, 375 (1981).
[30] K. Shimada, T. Sota, and K. Sizuki, J. Appl. Phys. **84**, 4951 (1998).
[31] K. Shimada, T. Sota, K. Sizuki, and H. Okumura, Jpn. J. Appl. Phys., Part 2 **37**, L1423 (1998).
[32] M. A. Littlejohn, J. R. Hauser, and T. H. Glisson, Appl. Phys. Lett. **26**, 625 (1975).
[33] A. S. Barker, Jr. and M. Ilegems, Phys. Rev. B **7**, 743 (1973).
[34] F. Bernardini and V. Fiorentini, Phys. Rev. Lett. **79**, 3958 (1997).
[35] J. W. Matthews and A. E. Blakeslee, J. Cryst. Growth **32**, 265 (1974).
[36] A. Fischer, H. Kuhne, and H. Richter, Phys. Rev. Lett. **73**, 2712 (1994).
[37] H. Angerer *et al.*, Appl. Phys. Lett. **71**, 1504 (1997).
[38] E. T. Yu, X. Z. Dang, L. S. Yu, D. Qiao, P. M. Asbeck, S. S. Lau, G. J. Sullivan, K. S. Boutros, and J. M. Redwing, Appl. Phys. Lett. **73**, 1880 (1998).
[39] A. J. Sierakowski and L. F. Eastman, J. Appl. Phys. **86**, 3398 (1999).
[40] B. E. Foutz, M. J. Murphy, O. Ambacher, V. Tilak, J. Smart, J. R. Shealy, W. J. Schaff, and L. F. Eastman, Mater. Res. Soc. Symp. Proc. **572** (in press).
[41] L. S. Yu, D. J. Qiao, Q. J. Xing, S. S. Lau, K. S. Boutros, and J. M. Redwing, Appl. Phys. Lett. **73**, 238 (1998).
[42] G. Martin, S. Strite, A. Botchkaev, A. Agarwal, A. Rockett, H. Morkoc, W. R. L. Lambrecht, and B. Segall, Appl. Phys. Lett. **65**, 610 (1994).
[43] G. Martin, A. Botchkarev, A. Rockett, and H. Morkoc, Appl. Phys. Lett. **68**, 2541 (1996).
[44] D. Brunner, H. Angerer, E. Bustarret, R. Höpler, R. Dimitrov, O. Ambacher, and M. Stutzmann, J. Appl. Phys. **82**, 5090 (1997).
[45] L. W. Wong, S. J. Cai, R. Li, K. Wang, H. W. Jiang, and M. Chen, Appl. Phys. Lett. **73**, 1391 (1998).
[46] A. D. Bykhovski, R. Gaska, and M. S. Shur, Appl. Phys. Lett. **73**, 3577 (1998).
[47] N. Maeda, T. Nishida, N. Kobayashi, and M. Tomizawa, Appl. Phys. Lett. **73**, 1856 (1998).
[48] S. Keller, G. Parish, P. T. Fini, S. Heikman, C.-H. Chen, N. Zhang, R. Vetury, S. P. DenBaars, and U. K. Mishra, ONR MURI Meeting, Panama City, FL, January 28th–29th, 1999.
[49] U. K. Mishra, Y.-F. Wu, B. P. Keller, S. Keller, and S. P. DenBaars, Phys. Semicond. Devices **1**, 878 (1998).
[50] Y.-F. Wu, B. P. Keller, S. Keller, D. Kapolnek, P. Kozodoy, S. P. DenBaars, and U. K. Mishra, Appl. Phys. Lett. **69**, 1438 (1996).
[51] J. Burm, W. J. Schaff, L. F. Eastman, H. Amano, and I. Akasaki, Appl. Phys. Lett. **68**, 2849 (1996).
[52] R. Gaska, A. Osinsky, J. W. Yang, and M. S. Shur, IEEE Electron Device Lett. **19**, 89 (1998).
[53] R. Gaska, J. W. Yang, A. Osinsky, Q. Chen, M. A. Khan, A. O. Orlov, G. L. Snider, and M. S. Shur, Appl. Phys. Lett. **72**, 707 (1998).
[54] S. C. Binari, J. M. Redwing, G. Kelner, and W. Kruppa, Electron. Lett. **33**, 242 (1997).
[55] E. T. Yu, X. Z. Dang, L. S. Yu, D. Qiao, P. M. Asbeck, S. S. Lau, G. J. Sullivan, K. S. Boutros, and J. M. Redwing, Appl. Phys. Lett. **73**, 1880 (1998).
[56] T. Wang, Y. Ohno, M. Lachab, D. Nakagawa, T. Shirahama, S. Sakai, and H. Ohno, Appl. Phys. Lett. **74**, 3531 (1999).
[57] N. G. Weimann, L. F. Eastman, D. Doppalapudi, H. M. Ng, and T. D. Moustakas, J. Appl. Phys. **83**, 3656 (1998).
[58] K. Leung, A. F. Wright, and E. B. Stechel, Appl. Phys. Lett. **74**, 2495 (1999).
[59] F. D. Sala, A. D. Carlo, P. Lugli, F. Bemardini, V. Fiorentini, R. Scholz, and J.-M. Jancu, Appl. Phys. Lett. **74**, 2002 (1999).
[60] S. S. Dhesi, C. B. Stagarescu, K. E. Smith, D. Doppalapudi, R. Singh, and T. D. Moustakas, Phys. Rev. B **56**, 10271 (1997).
[61] H. Amano, T. Takeuchi, S. Sota, H. Sakai, and I. Akasaki, Mater. Res. Soc. Symp. Proc. **449**, 1143 (1997).